

Neural Network Mapping and Clustering of Elastic Behavior from Tactile and Range Imaging for Virtualized Reality Applications

Ana-Maria Cretu, Emil M. Petriu and Pierre Payeur
School of Information Technology and Engineering
University of Ottawa
Ottawa, ON, Canada, K1N 6N5

Abstract – In order to fully reach its potential, virtualized reality needs to go beyond the modeling of rigid bodies and introduce accurate representations of deformable objects. This paper proposes an exploration of various image-based strategies that have been considered to address this issue and investigates into the intricate processes of acquisition and mapping of properties characterizing deformable objects. It applies an original neural network framework to characterize the relationship between surface deformation and forces exemplified in non-rigid bodies. The proposed network allows to map elastic behavior from data collected using a joint sensing strategy, combining tactile probing and range imaging. Beyond the complexity of the force/displacement relationship that can be encoded into the neural network without the need for sophisticated mathematical modeling tools, the neural network behaves as a guide for further probing by clustering measurements representing uniform elasticity regions. The sensor can therefore be readily directed toward areas of elasticity transitions where higher sampling density is required.

Keywords – Deformable objects, elasticity modeling, tactile sensing, range imaging, neural networks, probing guidance.

I. INTRODUCTION

The problem of sampling and modeling 3D elastic objects is subject to extensive research mainly resulting from the growing need to explicitly represent elastic behavior in a plethora of applications. However, the difficulties encountered in conducting strain-stress relationship measurements for objects made of materials that exhibit nonlinear behavior, the need for sophisticated equipment, and the complexity of developing relatively accurate material models introduce important challenges into this research effort.

In the majority of current applications, the selection of the physical constants is performed on the basis of a visual evaluation of the deformation of an object submitted to a given force, or numerical values are chosen according to some *a priori* knowledge regarding the material of which the object under measurement is made. There are four main categories of solutions encountered in the literature for gathering elastic behavior of objects: indentation [1, 2, 3, 4, 5, 6], vibration-based measurements [7], sound-based measurements [8, 9] and vision-based measurements [10, 11, 12, 13]. The most popular for daily engineering problems are indentation and vision-based measurements, while in medical applications, vibration and sound measurements are preferred due to the inaccessibility of measured organs.

This paper mainly addresses vision-based solutions to

measure elasticity. The principle usually employed is to collect a series of images before and after the deformation, analyze them individually and extract profiles in order to compute displacements that give a hint on the elastic properties of the objects. A point-wise correspondence is also needed between the deformed and undeformed profiles in order to compute the displacement. Several methods have been proposed for this purpose. Markers can be mounted directly on the objects [11, 12, 14], or the correspondence can be established using speckle patterns [15,16]. In the latter case, a thin film coating is applied on the surface of the object to generate the necessary speckle and the change of patterns with the deformation of the object is observed.

Wang *et al.* [14] use a grid of markers that also serves as nodes in a finite element–method model. Using digital image processing (corner extraction), the coordinates of various feature points in the grid and their displacement are obtained. From this information a strain field and the corresponding work-conjugate stress field are constructed and the forces are computed by balancing the internal stresses at each node. A similar idea is exploited by Kamiyama *et al.* [11, 12]. A tactile sensor, which uses a transparent elastic body with markers and a color CCD camera are employed to measure elastic behavior of objects. By taking images of a certain marker in the interior of an elastic body, the variation information of the interior is measured when a force is applied to the surface of an object that is considered homogeneous and with linear elasticity. The variation information of the interior is then used to reconstruct a force vector distribution. Vuskovic *et al.* [13] use a specially designed instrument to measure hyperelastic, isotropic materials, such as living tissues. The measurement method, based on pipette tissue aspiration, consists in leaning a tube against the tissue and gradually reducing the pressure in the tube. As the organ remains fixed to the tube, there are well-defined boundary conditions and a complete description of the deformation is given by the profile of the aspirated tissue. The measurements are done with a vision setup. An optical fibre illuminates the scene and the deformation is captured by a camera via a small mirror placed beside the aspiration hole. From the pictures, the material parameters are determined using the inverse finite element method. A Levenberg-Marquart parameter identification algorithm performs a minimization of the difference between the measured load-deformation data and the data obtained using the finite element method [13].

Ferrier *et al.* [15] and Hristu *et al.* [16] describe a deformable image-based tactile sensor consisting of a roughly elliptical membrane, filled with fluid-like gel and inscribed with a grid of dots at precisely computed locations of the inner surface of the membrane. A fibre optic cable illuminates the interior surface and images of the grid are taken as the membrane deforms. A solution for the 3D coordinates of the grid is obtained based on the assumption that the volume enclosed by the membrane remains constant, the boundary of membrane is fixed, and that the portion of the membrane which is not in contact will assume a shape that minimizes its elastic energy.

A neural-based solution without explicit computation of elasticity is presented by Greminger *et al.* [10], who take images after and before deformation to train a back-propagation neural network that defines the deformation of an elastic object submitted to an external force. The inputs to the network are the coordinates of a point in an undeformed body and the applied load on the body, and the outputs are the coordinates of the same point in the deformed body. The training data pairs are obtained directly from images of the object under known loads and therefore the neural network model is created without explicit computation of the elastic modulus. A computer vision deformable body tracking algorithm based on a boundary-element method is applied to measure the displacement of a point in the undeformed body.

The majority of these methods make the assumption that the material exhibits linear elastic behavior, that objects are homogeneous from the elasticity point of view, or make use of another method (e.g. finite element method, boundary element method) to recuperate the elasticity information and/or model the object. In this paper, an approach is investigated to develop a model that is not specific for a certain application, but provides a representation for different objects to be introduced in virtualized reality environments.

The proposed scheme leads to a model that is stand-alone and does not imply the use of heavy mathematical deformable objects representation techniques. Also, the neural architecture that is considered provides guidance toward the sampling points that are most relevant for a neural network to learn the elastic behavior of an object. This provides a critical advantage by allowing at the same time to model objects that have nonlinear elasticity and that can also be non-homogeneous. The modeling of elasticity is based on a separate neural network that stores the elasticity information without the need for recuperating elastic parameters explicitly.

While slightly similar from this perspective to the work of Greminger *et al.* [10], the proposed model is rather dedicated to build models of objects for virtualized reality applications and implies non-homogeneous objects that were not considered in the previous work. Here the interest is focused on the manner an object submitted to an external force deforms. Therefore, the elasticity neural network is analyzed from the perspective of being able to provide the deformation of a certain object as result of an interaction with a known force.

II. PROPOSED MODELING SCHEME

The proposed framework advantageously combines various neural network architectures to achieve diversified tasks as required for data collection and modeling of elastic characteristics. During the first phase, a non-uniform adaptive sampling algorithm based on a self-organizing neural architecture is implemented to selectively collect data only on those points that are relevant for mapping the elastic behavior of an object [17, 18]. Starting from a 3D point-cloud collected on an object or a scene of objects via an active range finder, a neural gas network obtains a compressed model for the dataset in which the weight vector consists of the 3D coordinates of the object's points. During the learning procedure, the model contracts asymptotically towards the points in the input space, respecting their density and thus taking the shape of the objects encoded in the point-cloud. These modeling properties ensure that the density of the tactile probing points is higher in the regions with more pronounced variations in the geometric shape. The advantage of such a model is not only to identify relevant sampling points, but also to allow for the determination of clusters of sampling points with similar geometric properties due to its ability to find an optimal finite set that quantizes the given input space. This provides a robust mechanism that can be extended to model non-homogeneous objects as well.

A feedforward neural network is then employed to model the force/displacement behavior of selected sampled points that are probed simultaneously by a force/torque sensor and the active range finder. Such an approach allows not only to recover the elastic parameters in the sampled points but also provides an estimate on the elastic behavior on surrounding points that are not part of the selected sampling point set. Fig. 1 illustrates the structure of the proposed approach.

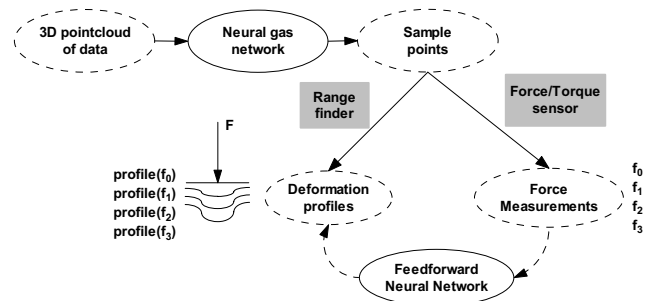


Fig. 1. Structure of the proposed neural-based sensing and mapping framework.

Using this selective data collection scheme, advantage is taken of the quantization properties of neural gas networks to split objects into clusters therefore insuring that different regions of possibly non-homogeneous objects are treated distinctly. Each cluster is sampled more than once, under the control of the selective sampling algorithm, in order to ensure enough data for an accurate representation of elasticity. This approach also copes with possible noise and errors induced by the measurement equipment.

III. FORCE/DISPLACEMENT ACQUISITION SETUP

Given that elastic constants are material-oriented parameters and do not accurately describe real-world objects in general, there is no attempt to explicitly recover elastic constants, nor stress or strain tensors for an object under loading. Instead, quantities of interest are those that can be observed on the surface of an object, namely the displacement of the surface as the object is loaded by a measured external force at a given point. The experimental setup used to collect force/displacement data is comprised of a multi-axis *ATI* force/torque sensor [19] attached to a console computer, an active triangulation line-scanning *Jupiter* laser range finder [20] controlled via a second PC system, as depicted in Fig. 2(a). The force/torque sensor is used to record the force components applied on the object while the range finder captures the deformation of the surface of the object under the given load. Fig. 2(b) illustrates the force/displacement data collection procedure on a deformable object representing one uniform cluster. The range finder is positioned such that the scanline intersects with the point where the external force is applied, as highlighted by the red trace of the laser on the object. At this stage of the work, the approach is validated on measurements taken with increasing forces applied perpendicularly to the surface of the object. Forces applied at different angles from the normal to the surface are not considered due to experimental constraints.

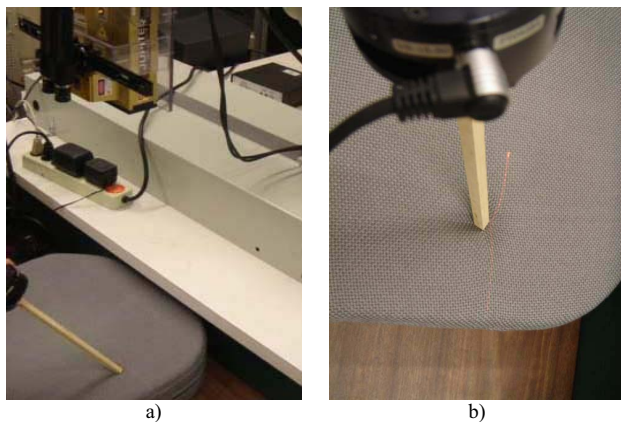


Fig. 2. a) Range sensor and force/torque setup producing b) a laser trace to capture object deformation resulting from the applied force.

The raw deformation profiles are encoded under the form of a 2D distribution of points in the Y - Z space, as shown in Fig. 3, where Y is the lateral displacement along the scanline and Z the depth along the optical axis with respect to a back reference plane. The laser range finder providing fast scan of 512 samples distributed along a straight line on the surface, 75 to 100 scans of the same area are collected within a few seconds while the applied force is kept constant. This provides efficient means to cope with the noise in the range data. Moreover, the success of the range data collection being highly sensitive to the texture and orientation of surfaces, missing measurements usually appear along the scan line.

The use of an iterative sampling procedure over a short period of time partially alleviates the impact of this constraint.

In order to filter out average noise and include as many valid measurements as possible in areas where points can be missing in some of the scans, the mean value is computed on the depth (Z -axis) over all deformation profiles obtained under a given force from the sampling points belonging to each cluster. The resulting profiles are then saved for each magnitude of normal force applied on the object and for each cluster of similar elasticity.

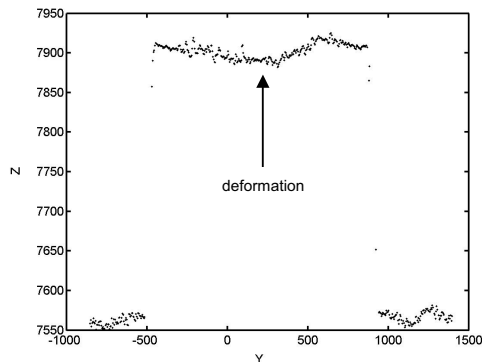


Fig. 3. A deformation profile mapped in the Y - Z space.

Given the nature of the modeling framework, there is no need to recuperate the explicit displacement information from the range profiles. Instead the neural network models the raw range data mapped in the Y - Z space as a function of applied force, F , without explicitly defining values for the displacement. For each cluster of similar elasticity, a feedforward neural network with two input neurons (Y and F), 25 hidden neurons (H_1 - H_{25}) and one output neuron (Z), as shown in Fig. 4, is employed to learn the relation between forces and the corresponding profiles provided by the range finder. One network is used to model the elastic behavior of each material (cluster). Once trained, the network tasks as inputs the Y coordinate and the force, F , and outputs the Z coordinate.

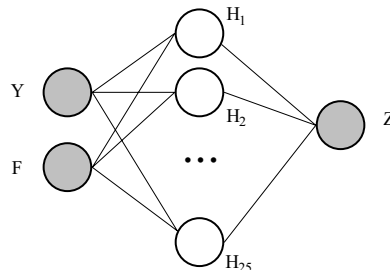


Fig. 4. Feedforward neural network to learn elastic behavior from deformation profiles under various force magnitudes.

The use of range profiles rather than full intensity images eases up the training procedure as only significant deformation features are retained. The dimensionality of the vision dataset is reduced to a vector, which can be directly fed into the neural network.

IV. EXPERIMENTAL RESULTS

In order to validate the proposed modeling framework, experimentation was conducted on a simple composite object made of a square cardboard box (medium elasticity) mounted on the top of a covered foam pillow (high elasticity), itself lying on a table top (no elasticity), as depicted in Fig. 5.



Fig. 5. Composite deformable object used for experimentation.

From the 3D point-cloud corresponding to the composite object initially obtained with a complete scan of its entire surface with the laser range finder, the neural gas network returns a set of significant sampling points, as shown in Fig. 6. Points located along the contours of each element of the composite object are automatically highlighted, thus providing immediate target areas for tactile probing with the force/torque sensor.

In this experimentation, the fact that objects were selected with different elastic characteristics helps study the case of objects with non-homogenous elastic behavior. The selected sampling points are clustered in two groups, corresponding to the two deformable materials. In Fig. 6, the blue points belong to the box, the red ones to the pillow. Force/displacement data is then collected for each of them, using the setup described in the previous section.

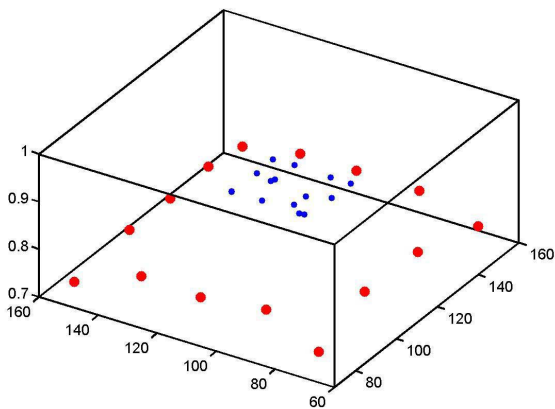


Fig. 6. Sampling points selected with the neural gas network.

Different magnitudes of a normal force are applied successively on the selected sampling points using the probe attached on the ATI force/torque sensor and an averaged range profile is collected with the laser range finder for each force magnitude. Fig. 7 and 8 show two examples of the

average deformation profiles resulting from the application of increasing forces. The first material, cardboard, depicted in Fig. 7 is semi-stiff, presenting symmetric deformation around the interaction point, while the second material, foam, shown in Fig. 8, is relatively smooth and exhibits a highly nonlinear elastic behavior, with asymmetric deformation profiles around the interaction point.

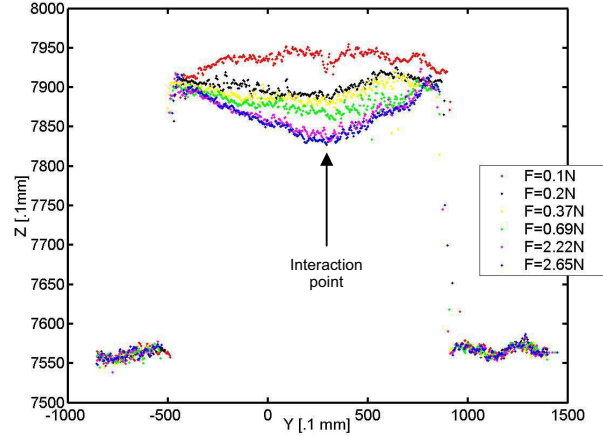


Fig. 7. Deformation profiles for semi-stiff material (cardboard).

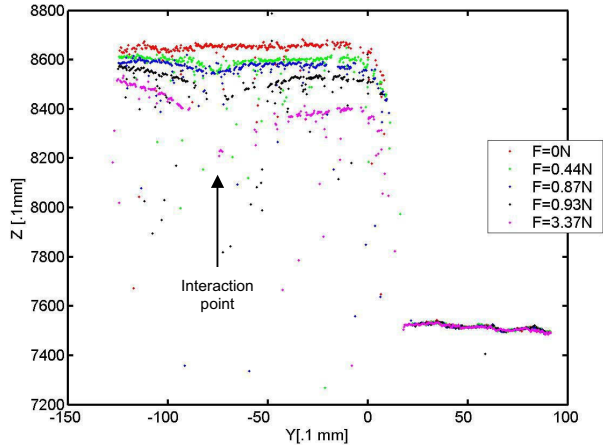


Fig. 8. Deformation profiles for smooth material (foam).

The point-wise correspondence required between the deformed and undeformed range profiles is insured by the fixed position of the range sensor and of the objects during data collection. As seen in Fig. 7 and 8, the range sensor data is more compact and less noisy for the semi-stiff material, while measurements get scattered on a wider range of values and exhibit a larger number of gaps in the case of the smooth material. This effect is mainly due to the rough texture of the fabric that covers the piece of foam. As the laser range finder operates on the principle of active triangulation, laser rays are expected to reflect on the object's surface before reaching back the sensor. When projected on a rough surface, laser rays are partially absorbed or diffused in all directions, depriving the range sensor from the expected echo or creating

false reflections that introduce errors on range estimation. This phenomenon gets amplified as the external force applied on a smooth object increases given that the orientation of the local surface is significantly modified.

Even though the data is noisy and contains important gaps for large forces, the network was trained directly with the averaged range profiles, as described section III, to avoid losing essential information. The only data processing applied is a normalization in the $[0 \ 1]$ interval prior to training, as required by the neural network implementation.

The networks associated with each material were trained for 10000 epochs using the Levenberg-Marquardt variation of the backpropagation algorithm [21], with the learning rate set to 0.09. The whole data set is used for training in order to provide enough samples. The training takes approximately 10 min. on a Pentium IV 1.3GHz machine with 512MB memory.

For the semi-stiff material, the mean square error reached during training is 3.50×10^{-7} , while for the smooth material it reached 1.78×10^{-5} . As expected, the error is lower for the first material where data is more compact and less noisy, while it remains slightly higher for the second material. But in both cases, excellent convergence is achieved.

The accuracy of the model is validated by the results obtained while testing the network for both materials. Fig. 9 presents the deformation characteristics for the semi-stiff material under the six different force magnitudes shown in Fig. 7. Fig. 10 presents corresponding characteristics for the smooth material submitted to a subset of force magnitudes shown in Fig. 8. In both figures, blue points represent the measured data and red points correspond to the estimation made by the neural network model under identical forces.

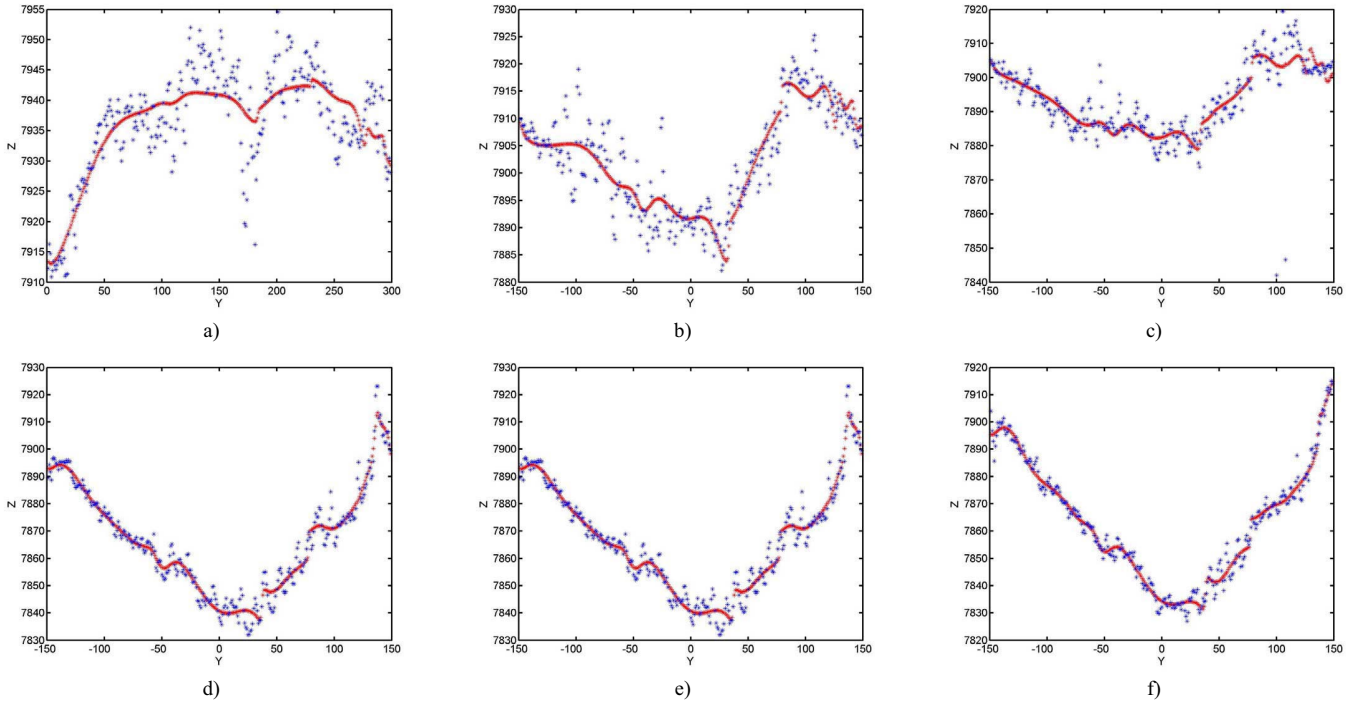


Fig. 9. Real and modeled deformation curves using neural network for semi-stiff material (cardboard) under a normal force of: a) $F=0.1N$, b) $F=0.2N$, c) $F=0.37N$, d) $F=0.69N$, e) $F=2.22N$, and f) $F=2.65N$.

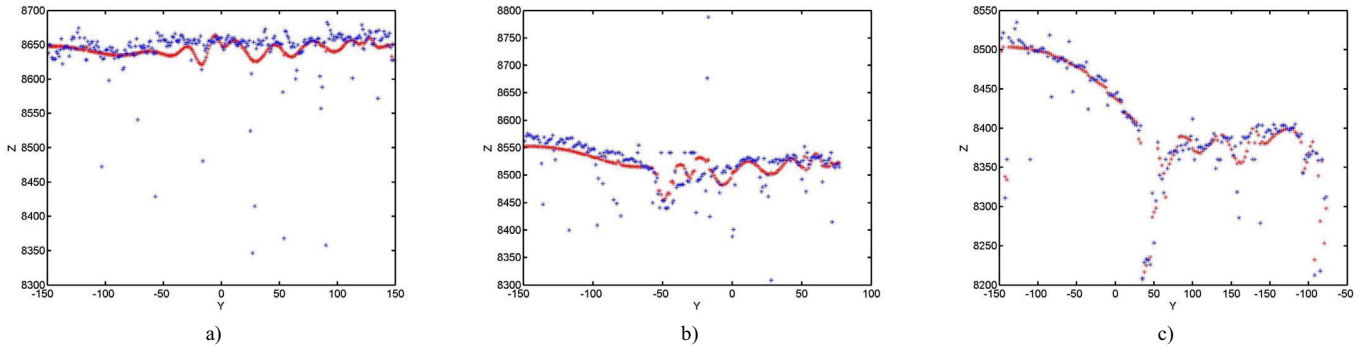


Fig. 10. Real and modeled deformation curves using neural network for smooth material (foam) under a normal force of: a) $F=0N$, b) $F=0.93N$, and c) $F=3.37N$.

REFERENCES

These curves demonstrate the high potential of neural networks in extracting the main features of highly nonlinear datasets, while being fault-tolerant and insensitive to noise inherently present in any real data. Sparse errors in the deformation profiles are successfully eliminated by the network. But the neural model remains fully capable of capturing the peak of the deformation profile, even in cases where the profile does not contain numerous sampling points, as exemplified in Fig. 10(c).

V. CONCLUSIONS AND FUTURE WORK

This investigation demonstrates that the benefit of using neural networks to model deformable objects is three-folded. First, neural networks provide continuous output behavior, thus being able to provide estimates for data that was not part of a training set. When compared with most of the work found in the literature where *a priori* knowledge about the characteristics of the material is assumed available, this paper proposes a robust approach for modeling force/deformation relationships from realistic experimental data with noisy and incomplete measurements, the latter being exemplified here by missing values for some of the points along the scan line.

Second, the use of a neural network modeling scheme avoids the complicated and frequently impossible to solve problem of recuperating explicit elastic parameters, especially for highly nonlinear elasticity. Finally, neural networks provide an accurate and fast response, without requiring the high computation times associated with the solving of mathematical models of deformable objects.

Combined with the neural gas network that reduces significantly the number of sample points needed to accurately represent a 3D deformable object, the proposed approach to model elasticity proves to be an efficient way to construct and represent elastic deformable objects since tactile probing on large surfaces would be prohibitive.

As future work, we plan to enhance the accuracy of the proposed approach by collecting data for different angles of force application, and add these angles as supplementary inputs in the network. This would improve the modeled behavior especially for objects exhibiting highly nonlinear characteristics. We also plan to extend the study of the performance of the approach to other objects.

ACKNOWLEDGEMENTS

This work was funded in part by the Communications and Information Technology Ontario Centre of Excellence (CITO), and by the Materials and Manufacturing Ontario Centre of Excellence (MMO). Authors also wish to acknowledge support from the Ontario Graduate Scholarship program.

- [1] D. Aulignac, C. Laugier, M.C. Cavusoglu, "Towards a Realistic Echographic Simulator with Force Feedback", *Proc. IEEE/RSI Int. Conf. Intelligent Robots and Systems*, Korea, pp. 727-732, 1999.
- [2] C. Monserrat, U. Meier, M. Alcañiz, F. Chinesta, M.C. Juan, "A New Approach for the Real-Time Simulation of Tissue Deformations in Surgery Simulation", *Computer Methods and Programs in Biomedicine*, vol. 64, issue 2, pp. 77-85, 2001.
- [3] D. K. Pai, K. van den Doel, D. L. James, J. Lang, J. E. Lloyd, J. L. Richmond, S. H. Yau, "Scanning Physical Interaction Behavior of 3D Objects", *Proc. 28th annual conference on Computer graphics and interactive techniques*, pp. 87-96, 2001.
- [4] H.T. Tanaka, K. Kushihamana, N. Ueda, "A Vision-based Haptic Exploration", *Proc. IEEE Int. Conf. Robotics & Automation*, Taiwan, pp. 3441-3448, 2003.
- [5] K.K. Tho, S. Swaddiwudhipong, Z.S. Liu, J. Hua, "Artificial Neural Network Model for Material Characterization by Indentation", *Modeling and Simulation in Material Science and Engineering*, no.12, pp. 1055-1062, 2004.
- [6] N. Ueda, S. Hirai, H.T. Tanaka, "Extracting Rheological Properties of Deformable Objects with Haptic Vision", *Proc. IEEE Int. Conf. Robotics & Automation*, pp. 3902-3907, 2004.
- [7] A.M. Okamura, J. T. Dennerlein, R.D. Howe, "Vibration Feedback Models for Virtual Environments", *Proc. IEEE Int. Conf. Robotics and Automation*, pp. 1- 6, 1998.
- [8] Y. Zhu, T.J. Hall, J. Jiang, "A Finite-Element Approach for Young's Modulus Reconstruction", *IEEE Trans. Med. Imaging*, vol. 22, no.7, pp. 890-901, 2003.
- [9] J. Li, M. Wan, M. Qian, J. Cheng, "Elasticity Measurement of Soft Tissue Using Shear Acoustic Wave and Real-Time Movement Estimating Based on PCA Neural Network", *Proc. Int. Conf. IEEE Eng. in Medicine and Biology Soc.*, vol. 3, pp. 1395-1396, 1998.
- [10] M. A. Greminger, B. J. Nelson, "Modeling Elastic Objects with Neural Networks for Vision-Based Force Measurement", *Proc. Int. Conf. Intelligent Robots and Systems*, pp. 1278-1283, 2003.
- [11] K. Kamiyama, H. Kajimoto, M. Inami, N. Kawakami, S. Tachi, "A Vision-based Tactile Sensor", *Proc. Int. Conf. Artificial Reality and Telexistence*, pp. 127- 134, 2001.
- [12] K. Kamiyama, H. Kajimoto, N. Kawakami, S. Tachi, "Evaluation of a Vision-based Tactile Sensor", *Proc. IEEE Int. Conf. Robotics & Automation*, pp. 1542- 1547, vol. 2, 2004.
- [13] V. Vuskovic, M. Krauer, G. Szekeley, M. Reidy, "Realistic Force Feedback for Virtual Reality Based Diagnostic Surgery Simulators", *Proc. IEEE Int. Conf. Robotics & Automation*, pp. 1592-1598, 2000.
- [14] X. Wang, G.K. Ananthasuresh, J.P. Ostrowski, "Vision-based Sensing of Forces in Elastic Objects", *Sensors and Actuators A*, vol.94, pp.146-156, 2001.
- [15] N. J. Ferrier, R. W. Brockett, "Reconstructing the Shape of a Deformable Membrane from Image Data," *Int. Journal Robotics Research*, vol. 19, no. 9, pp. 795-816, 2000.
- [16] D. Hristu, N. Ferrier, R. W. Brockett, "The Performance of a Deformable-membrane Tactile Sensor: Basic Results on Geometrically-defined Tasks," *Proc. IEEE Int. Conf. Robotics & Automation*, 2000.
- [17] A.-M. Cretu, E.M. Petriu, G.G.Patry, "Neural-Network Based Models of 3D Objects for Virtualized Reality: A Comparative Study", *IEEE Trans. Instr. & Meas.*, vol.55, no.1, pp. 99-111, Feb. 2006.
- [18] A.-M. Cretu, J. Lang, E.M. Petriu, "Adaptive Acquisition of Virtualized Deformable Objects with a Neural Gas Network", *Proc. IEEE Int. Workshop on Haptic, Audio-Visual Environments and their Applications*, Ottawa, Ontario, pp. 165-170, 2005.
- [19] ATI Industrial Automation Inc, *Installation and Operations Manual for Stand-Alone F/T Sensor Systems*, Garner, NC, 1997.
- [20] Servo-Robot Inc, *Jupiter 3-D Laser Vision Camera Installation and Operation Manual*, St-Bruno, QC, 1996.
- [21] M.T.Hagan, H.B. Demuth, M. Beale, *Neural Network Design*, PWS Publishing Company, USA, 1996.